

Predicting Dissolution of Entecavir Using the Noyes Whitney Equation

Yanlei Kang¹, Jiahui Chen¹, Zhenyu Duan¹, and Zhong Li^{1*}

¹Zhejiang Province Key Laboratory of Smart Management & Application of Modern Agricultural Resources, School of Information Engineering, Huzhou University, Huzhou, Zhejiang, China.

email: lizhong@zjhu.edu.cn

ABSTRACT

The dissolution rate of a drug directly affects its absorption and utilization in vivo. The dissolution test is used to evaluate the quality of formulation and production process. Entecavir is approved by the United States FDA for the treatment of chronic hepatitis B. Entecavir monohydrate (ETV-H) is used in commercial ETV tablets. The anhydrous form of entecavir (ETV-A) often appears as an impurity polymorph during the preparation process. This study aims to investigate the dissolution behavior of ETV-H in four dissolution media (water, pH 1.2, pH 4.0, and pH 6.8) and compare with those of ETV-A. The dissolution rates of ETV-H at pH 6.8, pH 4.0, and ultrapure water were faster than those of ETV-A, resulting in faster complete dissolution of ETV-H. To save time in the dissolution testing, an analytical method based on the Noyes Whitney equation is proposed to obtain the fitted (predicted) dissolution curve. Differences (loss values) between the predicted and experimental dissolution curves for ETV-H at pH 6.8 and pH 1.2 were 0.0013 and 0.016, respectively. The proposed analytical method can save up to 75% of experimental time and can be used for dissolution testing of active pharmaceutical ingredients in the production of pharmaceutical crystals.

KEYWORDS: dissolution, analytical method, entecavir, Noyes-Whitney equation

INTRODUCTION

Drug dissolution refers to the rate and extent of drug release from solid preparations (such as tablets, capsules, or granules) in a specific medium (1). Because the dissolution rate directly affects the absorption and utilization of drugs in vivo, the dissolution test has become one of the indicators to evaluate the quality of drug production (2–4). Dissolution is widely used in the development of solid dosage forms, raw materials, and new drugs (5, 6). The main factors affecting dissolution are variations in the crystalline form, preparation form, formulation and excipients, manufacturing process, and drug interactions (7–9). The surface free energy of different crystal forms affects the dissolution rate and bioavailability of drugs. Studies have shown that different crystalline forms of the same drug have different absorption in vivo (10, 11). Dissolution is an important quality control indicator used to evaluate the consistency of different production batches. The dissolution test is applicable not only to solid dosage forms but also to active pharmaceutical ingredients (APIs) (12).

The United States FDA approved Entecavir (ETV) (Baraclude, Bristol-Myers Squibb Co. Ltd) for the treatment of chronic hepatitis B in 2005 (12). ETV is a carbocyclic 2'-deoxyguanosine analogue, which can phosphorylate into a triphosphate form that can inhibit hepatitis B virus (HBV) in active cells (13). ETV is chemically defined as 2-amino-1, 9-dihydro-9-((1S,3R,4S)-4-hydroxy-3-(hydroxymethyl)-2-methylenecyclopentyl)-6H-purin-6-one. Entecavir monohydrate (ETV-H) is the API used in commercial ETV tablets (14). As a polymorphic impurity of ETV-H, entecavir anhydrate (ETV-A) may occur in the ETV-H production process (15).

Most patients who take ETV are elderly or infirm, and the pH value and motility of the gastrointestinal environment are quite different from those of young people. To investigate the dissolution of ETV-H and ETV-A, four dissolution media with pH values of 1.2, 4.0, 6.8, and 7.0 (ultrapure water) were selected for this study. The dissolution medium at pH 1.2 was usually used to simulate the gastric acid environment, pH 4.0 was used to simulate the gastric environment of elderly or weak patients, and

*Corresponding author

pH 6.8 was used to simulate intestinal environment.

In previous literature, the dissolution of ETV-H was investigated by HPLC (16, 17) and Raman spectroscopy (18). In this paper, the dissolution of ETV-H was investigated with UV-Visible spectrophotometry. To save time with dissolution testing of APIs with polymorphic impurities such as ETV, an analytical method based on the Noyes Whitney equation was developed. The method was validated with dissolution of ETV-H in different media.

MATERIALS AND METHODS

Materials

ETV-H was obtained from Zhejiang Ausun Pharmaceutical Co., LTD (purity > 99.9%). ETV-A was recrystallized by dissolving ETV-H solid powder in a methanol solvent using a cooling crystallization method. Standard Entecavir (Batch No. 101248-201503) was purchased from China Institute for Food and Drug Control, and the calculated C₁₂H₁₅N₅O₃ content was 93.8%.

Hydrochloric acid (HCl), potassium hydroxide (KOH), sodium dihydrogen phosphate (NaH₂PO₄), sodium hydroxide (NaOH), acetic acid (CH₃COOH), sodium acetate (CH₃COONa), potassium chloride (KCl), and boric acid (H₃BO₃) were used for solubility and dissolution determination. All reagents were purchased from Aladdin Ltd. (Shanghai, China), were of analytical grade, and were used without further purification. Ultrapure water was prepared by Arium Mini ultrapure water system (Sartorius, Goettingen, Germany).

Preparation of Tablets for Dissolution Determination

ETV-H powder and ETV-A powder (150 mg of each crystal form) were pressed respectively for 1 minute with YP-15 manual powder tablet press (Tianjin Zhongshi JOSVOK Technology Development Co., Ltd., China). The tablet diameter was 10 mm, and the pressure was 25 MPa. The measured thickness of the compressed tablet was about 1 mm. A total of 12 tablets were pressed for each crystal form.

All weighing operations were performed in XS205DU electronic balance (METTLER TOLEDO Instrument Co., Ltd, Switzerland) with an accuracy of 0.01 mg.

Preparation of Dissolution Media

The HCl solution at pH 1.2 was prepared according to the *Chinese Pharmacopoeia* (ChP). HCl with a mass concentration of 37% (7.65 mL) was transferred to a 1000-mL volumetric flask, then ultrapure water was added to the tick mark.

The acetate buffer solution at pH 4.0 was prepared

according to ChP. Acetic acid (114 mL) was added to a 1000-mL volumetric flask, then ultrapure water was added to tick mark to obtain a 2 mol/L solution. Sodium acetate (1.22 g) and the acetic acid solution (20.5 mL) were added to a 1000-mL volumetric flask, and then ultrapure water was added to the tick mark.

To prepare the phosphate buffer solution at pH 6.8, NaOH (8.0 g) was transferred to a 1000-mL volumetric flask and ultrapure water was added to the constant volume to obtain the NaOH solution with a concentration of 0.2 mol/L. Potassium dihydrogen phosphate (6.8 g) and sodium hydroxide solution (0.2 mol/L, 112 mL) were transferred to a 1000-mL volumetric flask, and then ultrapure water was added to dilute to the constant volume.

All dissolution media were degassed under vacuum before use with a ZKT-18F vacuum degasser (Tianjin Tianda Tianfa Technology Co., Ltd.) at 0.05 MPa vacuum degree for 30 minutes.

Dissolution Experiments

To obtain the dissolution curves for comparison of the two substances, we used the same weight of ETV-A and ETV-H. The moles of ETV in ETV-A and ETV-H were not the same, so, the UV spectrum of ETV-H and ETV-A was slightly different.

Standard Entecavir (7.5mg) was added to a 250-mL volumetric flask, diluted with ultrapure water to volume. A solution with a concentration of 30 µg/mL was obtained. Then the solution was diluted to a series of ETV-H solutions with concentration of 25, 20, 15, 10, and 5 µg/mL. According to the content of C₁₂H₁₅N₅O₃ in standard entecavir (93.8%), a series of ETV-A solutions were prepared with concentrations of 30, 25, 20, 15, 10, and 5 µg/mL. All standard solutions of ETV-H and ETV-A were measured at 253 nm against blank solution to obtain absorbance, and each concentration was measured three times. Finally, the standard curves of ETV-H and ETV-A were plotted according to the UV absorption intensity at 253 nm of different concentrations (Figs. 1c and 1d). The UV spectrum of ETV-H and ETV-A in HCl solution is shown in Figure 1e, and the absorption peaks of ETV-H and ETV-A appeared at 255 nm (the standard curves are shown in Figs. 1f and 1g). The absorption peaks of ETV-H and ETV-A at pH 4.0 and 6.8 were consistent with that in water. The standard curves of ETV-H and ETV-A in pH 4.0 and pH 6.8 were also obtained referred to the above method (not shown).

All dissolution experiments were performed using the

paddle dissolution apparatus and RCZ-8M drug dissolution meter (Tianjin Tianda Tianfa Technology Co., Ltd., China), which had eight dissolution vessels (1000-mL capacity) and eight paddle shafts. Concentration of the solution was analyzed with a Cary 60 UV-Vis spectrophotometer (Agilent, USA).

The dissolution tests were conducted at $37 \pm 0.5^\circ\text{C}$ with a speed of 250 rpm in 900 mL of dissolution media. Samples (5 mL) were withdrawn at different time points and filtered through 0.45- μm nylon filters (Sarrtorius, Germany). The dissolution medium was replaced with the same temperature and volume (5 mL). Then samples were analyzed at the wavelength of 253 nm by the UV-Vis spectrometer. Experiments were conducted in triplicate, and the relative standard deviation (RSD%) value was calculated at each time point. The concentration at each time point was obtained according to the standard curve. The experiment was stopped when ETV-H or ETV-A tablets were completely dissolved.

The analytical method was performed using Matlab R2017b (Mathworks Inc., MA, USA).

Characterization of Entecavir Polymorphs

ETV-H and ETV-A were characterized by powder x-ray diffraction (PXRD) to verify the purity of both crystal forms. A Rigaku D/Max-2550 powder diffractometer (Rigaku Co., Japan) was used, with a $\text{CuK}\alpha$ radiation source, $\lambda = 1.54059\text{\AA}$, at 40 kV and 250 mA. The scans ran from 3.0° to 50.0° (2θ), with an increasing step size of 0.02° (2θ) and count time of 2 s per step. Data were processed using MDI Jade software (version 9.0).

RESULTS AND DISCUSSION

Calibration Curve

The PXRD results of ETV-H and ETV-A showed that these two crystal forms had distinct characteristic peaks (Fig. 1a). ETV-H and ETV-A had no change in crystal form after tablet pressing. Both ETV-H and ETV-A had UV absorption peaks at 253 nm (Fig. 1b).

Dissolution Curves

The dissolution test results are shown in Figure 2.

At pH 1.2, the sampling time points were 3, 6, 9, 12, 15, 20, 25, 30, 35, 40, 50, 60, 70, 80, and 90 minutes (Fig. 2a). The dissolved amount of ETV-H and ETV-A both reached 90% at 15 minutes, indicating rapid dissolution at pH 1.2. There was no significant difference in the dissolution rate between ETV-H and ETV-A.

At pH 4.0, the sampling time points were 3, 5, 10, 15, 20, 25, 30, 40, 50, 60, 70, 80, 100, 120, 140, 160, 180, 200, 220,

240, 280, 300, and 320 minutes (Fig. 2b). The cumulative release of ETV-H exceeded 90% at 120 minutes and 99% at 180 minutes. The cumulative dissolution of ETV-A exceeded 90% at 240 minutes and 99% at 300 minutes. The dissolution rate of ETV-H at pH 4.0 was faster than that of ETV-A.

At pH 6.8, the sampling time points were 3, 5, 10, 15, 20, 25, 30, 40, 50, 60, 70, 80, 90, 100, 120, 140, 160, 180, 200, 220, 240, 260, 280, 300, 320, 340, and 360 minutes (Fig. 2c). The cumulative release of ETV-H was over 90% at 160 minutes and 99% at 260 minutes. The dissolution of ETV-A exceeded 90% at 220 minutes and 99% at 260 minutes. At pH 6.8, ETV-H dissolved faster than ETV-A before cumulative drug release reached 90%.

In ultrapure water, the sampling time points were 3, 5, 10, 15, 20, 25, 30, 35, 40, 50, 60, 70, 80, 90, 100, 110, 120, 160, 180, 200, 220, 240, 260, 280, 300, and 320 minutes (Fig. 2d). The cumulative release of ETV-H and ETV-A exceeded 90% at 140 and 220 minutes, respectively, and complete dissolution was reached at 160 and 280 minutes, respectively. The dissolution rate of ETV-H was faster than that of ETV-A in pure water.

To sum up, under the same experimental conditions, the dissolution rate of ETV-H was higher than that of ETV-A in dissolution medium of pH 4.0, pH 6.8, and ultrapure water. The dissolution profiles at pH 1.2 differed from those at pH 4.0, pH 6.8, and ultrapure water, which may be due to the protonation of ETV in the dissolution medium at pH 1.2 (19). Therefore, after the API dissolved at pH 4.0, pH 6.8, and in ultrapure water, the pH value of the dissolution solution remained constant, and the pH of dissolution medium may change at pH 1.2.

Analytical Method for Predicting the Dissolution Curve

The earliest report of the dissolution rate equation was jointly proposed by Noyes and Whitney in 1897 (20).

During the dissolution process of the drug, the surface area of the drug is constantly changing. Assuming that the initial volume of the tablet is V_t , and the volume of drug dissolved in the dissolution medium at time t is V_d , then, during the drug dissolution process, the undissolved solid volume of the drug at time t is $V_u = V_t - V_d$. Dissolved solid volume correlates with the drug surface area.

When the drug is a cylindrical solid tablet, the tablet's surface area is $S = \pi r^2 + 2\pi r h$, and the tablet's volume is $\pi r^2 h$, where r represents the radius of the bottom surface of the tablet, and h is the height of the tablet. Assuming that the height of the tablet is βr , then $S = \pi r^2 (1 + 2\beta)$ and

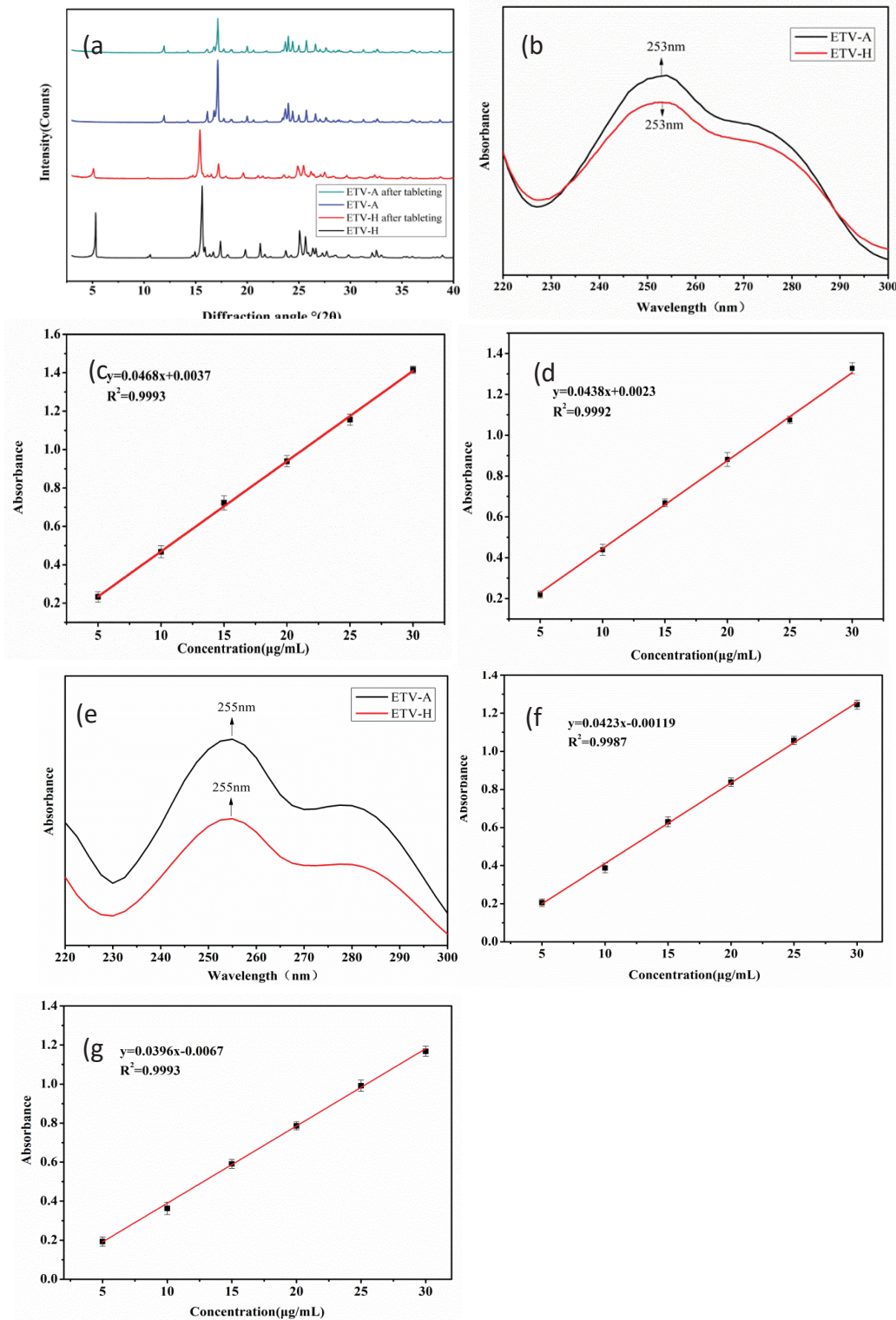


Figure 1. Powder x-ray diffraction of ETV-A and ETV-H (a); UV spectra of ETV-A and ETV-H in water (b); UV absorption standard curve of ETV-A in water (c); UV absorption standard curve of ETV-H in water (d); UV spectra of ETV-A and ETV-H at pH 1.2 (e); UV absorption standard curve of ETV-A at pH 1.2 (f); and UV absorption standard curve of ETV-H at pH 1.2 (g). ETV-A: entecavir anhydrate; ETV-H: entecavir monohydrate; UV: ultraviolet.

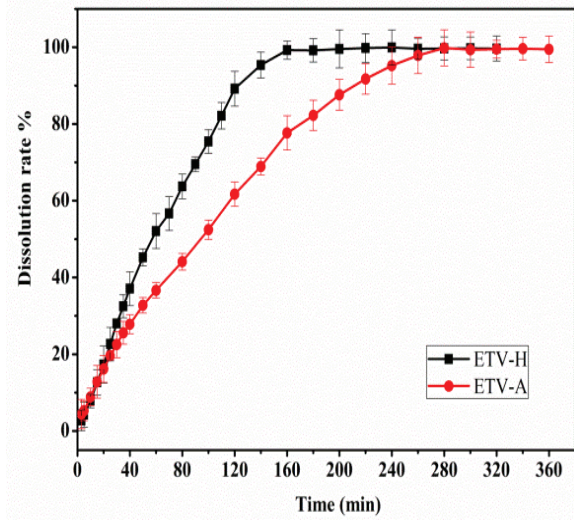
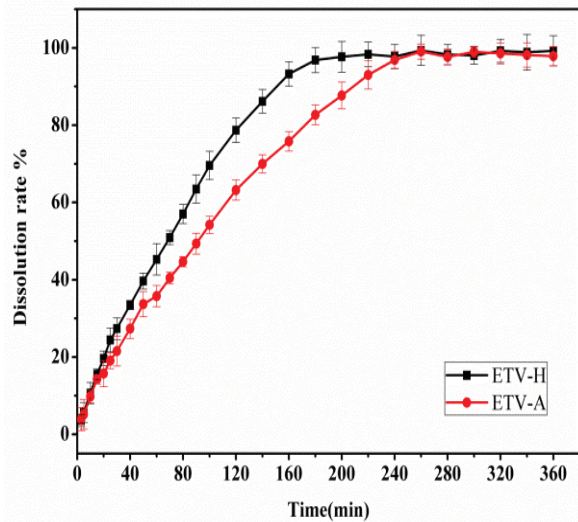
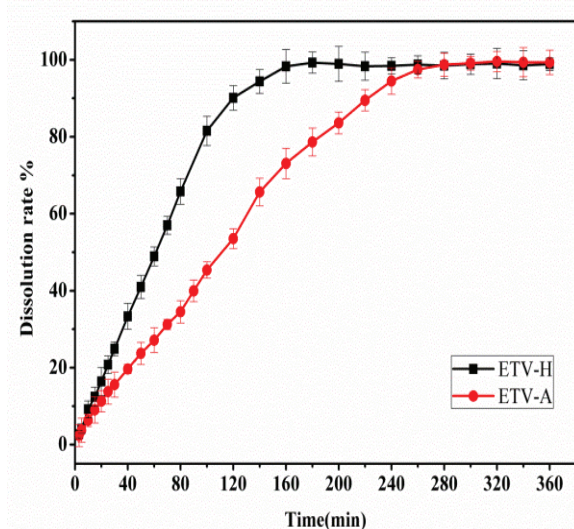
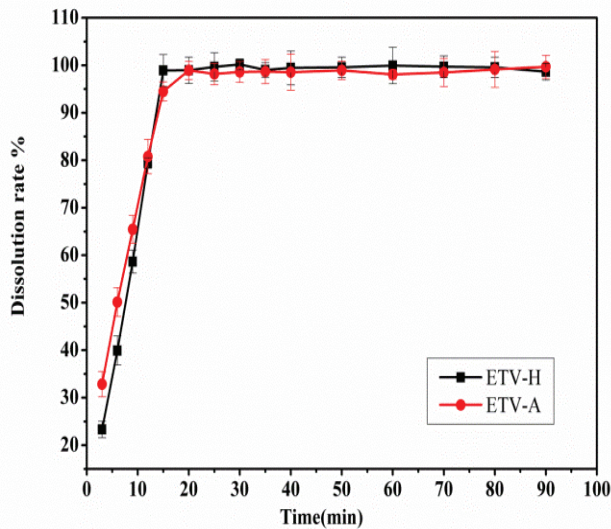


Figure 2. Dissolution curves of ETV-H and ETV-A at pH 1.2 (a), pH 4.0 (b), pH 6.8 (c), and in pure water (d). ETV-A: entecavir anhydrate; ETV-H: entecavir monohydrate.

$V_t = \pi r^2 \times \beta r$. Then $r = (V_t / \pi\beta)^{2/3}$. The tablet surface area can be expressed as $S = 2\pi (1 + 2\beta) (V_t / \pi\beta)^{2/3}$. If $\alpha = 2\pi (1 + 2\beta) (1 / \pi\beta)^{2/3}$, then S is transformed to $S = \alpha (V_t)^{2/3}$.

If the volume of the tablet remains a cylinder during the dissolution process, then the Noyes-Whitney equation is converted into:

$$\frac{dC}{dt} = k\alpha(V_t - V_d)^{2/3}(C_s - C_t), \quad \text{Eq. (1)}$$

where C_s refers to the saturated solubility of the drug, k is the dissolution rate constant, S means the surface area of the drug, and C_t denotes the solubility of the drug in the solvent at time t , which is the instantaneous concentration. At time t , V_d is determined by C_t , the tablet density ρ , and solvent volume V_s . Then Eq. (1) is converted as follows:

$$\frac{dC}{dt} = k\alpha\left(\frac{V_t \times \rho}{V_s} - C\right)^{2/3}\left(\frac{V_s}{\rho}\right)^{2/3}(C_s - C_t), \quad \text{Eq. (2)}$$

Assuming that the concentration of the drug after complete dissolution in the dissolution medium is C_d , it can be calculated by the following equation: $C_d = (V_t \times \rho) / V_s$. Then Eq. (2) can be transformed into:

$$\frac{dC}{dt} = k\alpha(C_d - C)^{2/3}\left(\frac{V_s}{\rho}\right)^{2/3}(C_s - C_t), \quad \text{Eq. (3)}$$

During the dissolution process, V_s is always 900 mL by replenishing the solution. So, in Eq. (3), k , α , V_s , ρ are constants. If $K = k\alpha (V_s / \rho)^{2/3}$, then Eq. (3) can be converted to:

$$\frac{dC}{dt} = K(C_d - C)^{2/3}(C_s - C_t), \quad \text{Eq. (4)}$$

where K is a constant. The key to solving Eq. (4) is to find the value of K . The analytical method refers to predicting the whole dissolution curve through a small amount of dissolution test data using Eq. (4), which is derived from the Noyes Whitney equation.

As an example, the dissolution data of ETV-H in the pH 6.8 medium at different time points (including the time point and drug concentration in the dissolution medium at this time point) were imported into Matlab. The K value in the dissolution curve was obtained by selecting the data for a certain number of time points, then K was substituted into Eq. (4) as follows.

According to the existing literature, the saturated solubility of ETV-H in the dissolution medium of pH 6.8 is 2.5 mg/mL at 37 °C (19). Saturated solubility can be calculated as follows. Assume that the drug concentration in the dissolution medium is C_{t1} at time $t1$ and C_{t2} at time $t2$. Then the concentration difference is divided by the time difference to get the dissolution rate $k1$ between two adjacent points, which is equal to the dC / dt value: $k1 = dC / dt = (C_{t2} - C_{t1}) / (t2 - t1)$. The constant K in Eq. (4) is calculated as $K = k1 / (C_d - C_{t1})^{2/3}(C_s - C_{t1})$. The constant K between time $t1$ and $t2$ is $k1$. It can be inferred that between time $t2$ and time $t3$, the constant K is $k2$, and the constant K between time $t-1$ and time t is $kt-1$. Substituting $k1, k2, \dots, kt-1$, the obtained average value is equal to K in Eq. (4), and the fitted dissolution curve can be obtained. During the calculation, the dissolution curve obtained from K fluctuates in the instantaneous concentration values near the time point of complete dissolution. Thus, Eq. (4) can be converted to:

$$\frac{dC}{dt} = K(C_d - C)^{\frac{2}{3}}(C_s - C_t) \quad \text{Eq. (5)}$$

By comparing the fitted (predicted) curve with the actual (experimental) dissolution curve, the sum of the squares of the concentration difference between the two curves can be obtained. The number of data points corresponding to the smallest loss value can be chosen as the optimal number of samples to predict the dissolution curve.

Figure 3 shows the comparison between the predicted and experimental curves for ETV-H at pH 6.8. When the number of data points was eight (i.e., 3, 5, 10, 15, 20, 25, 30, and 40 min), the loss value was the smallest at 0.0013. At this point, the predicted curve was closest to the experimental curve. For these eight data points, the calculated average K value was 0.00195, and the standard deviation was 2.66×10^{-5} .

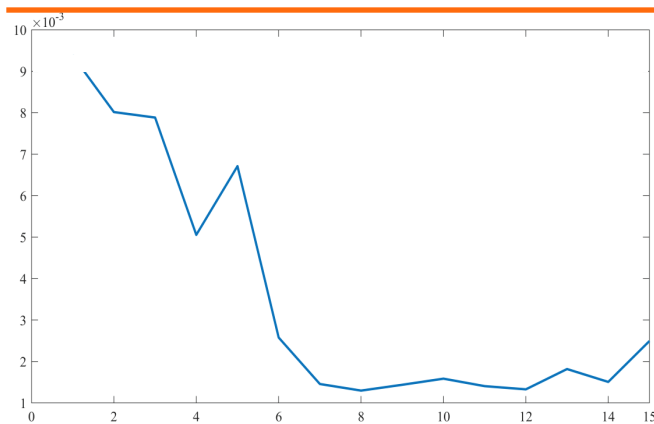


Figure 3. Determination of required number of experimental data points needed to predict the dissolution curve for ETV-H at 6.8. Loss values reflect differences between fitted (predicted) and actual (experimental) results. ETV-H: entecavir monohydrate.

As shown in Figure 4, the predicted dissolution curve tended to agree with the actual dissolution curve at pH 6.8. Therefore, only the dissolution sampling results within 40 minutes were needed to obtain the predicted dissolution profile according to Eq. (5). Thus, this analytical method can greatly reduce the experimental time.

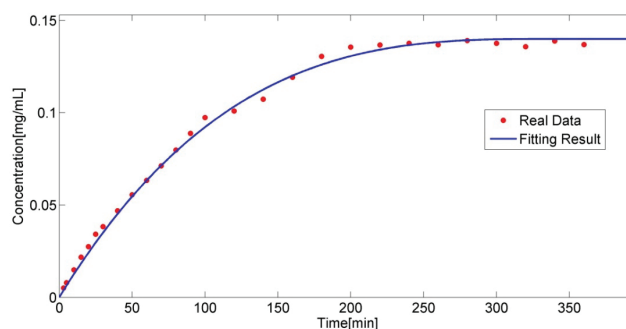


Figure 4. Comparison of predicted dissolution curve (blue line) and experimental results (red dots) of ETV-H in pH 6.8. ETV-H: entecavir monohydrate.

For the dissolution of ETV-H at pH 1.2, the loss value between the predicted with actual dissolution curve was obtained by selecting different data points. As shown in Figure 5, the loss value was the smallest (0.016) when taking the first four experimental data (i.e., 3, 6, 9, 12 min). These four data points were used to predict and fit the dissolution curve, as shown in Figure 6. The average K value was 0.002, and the standard deviation was 6.67×10^{-5} . The predicted dissolution curve was in good agreement with the experimentally obtained dissolution curve. The saturated solubility of ETV-H was approximately 25 mg/mL at 1.2 at 37 °C (19).

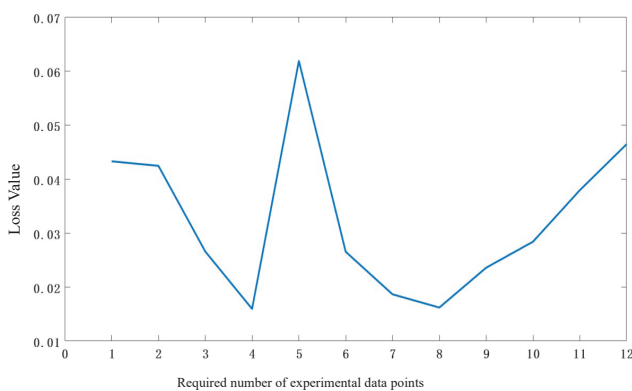


Figure 5. Determination of required number of experimental data points needed to predict the dissolution curve for ETV-H at 1.2. Loss values reflect differences between fitted (predicted) and actual (experimental) results. ETV-H: entecavir monohydrate.

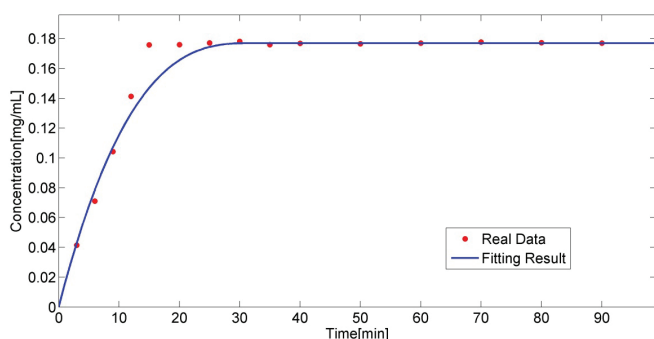


Figure 6. Comparison of predicted dissolution curve (blue line) and experimental results (red dots) of ETV-H at pH 1.2. ETV-H: entecavir monohydrate.

CONCLUSIONS

The dissolution behavior of ETV-H in four dissolution media was comprehensively investigated and compared with that of ETV-A. The dissolution rate of ETV-H in pH 6.8, pH 4.0, and ultrapure water was faster and the complete dissolution time was shorter than that of ETV-A. A soft-sensor analytic method for predicting the ETV-H dissolution curve using the Noyes Whitney equation was proposed. The dissolution curves of ETV-H in acidic and weak alkaline media (pH 6.8 and 1.2) were predicted. The predicted curves were consistent with the experimental results, differences (loss values) of 0.0013 and 0.016 at pH 6.8 and 1.2, respectively. This dissolution test method can save up to 75% of the experimental time for dissolution testing of bulk APIs.

FUNDING

This work was supported by the National Natural Science Foundation of China (no. 12171434), the State Key Laboratory of Industrial Control Technology (open project no. ICT2021B55), and Zhejiang Provincial Department of Education (research project no. Y202146004).

CONFLICT OF INTERESTS

The authors disclosed no conflicts of interest related to this article.

REFERENCES

- Gao, Y.; Glennon, B.; He, Y.; Donnellan, P. Dissolution kinetics of a BCS class II active pharmaceutical ingredient: diffusion-based model validation and prediction. *ACS Omega* **2021**, *6* (12), 8056–8067. DOI: 10.1021/acsomega.0c05558.
- Li, J.; Spivey, N.; Silchenko, S.; Gonzalez-Alvarez, I.; Bermejo, M.; Hidalgo, I. J. A differential equation based modelling approach to predict supersaturation and in vivo absorption from in vitro dissolution-absorption system (idas2) data. *Eur. J. Pharm. Biopharm.* **2021**, *165*, 1–12. DOI: 10.1016/j.ejpb.2021.05.003.
- Thakore, S. D.; Sirvi, A.; Joshi, V. C.; Panigrahi, S. S.; Manna, A.; Singh, R.; Sangamwar, A. T.; Bansal, A. K. Biorelevant dissolution testing and physiologically based absorption modeling to predict in vivo performance of supersaturating drug delivery systems. *Int. J. Pharm.* **2021**, *607* (7), 120958. DOI: 10.1016/j.ijpharm.2021.120958.
- Tung, N. T.; Tran, C. S.; Nguyen, T. L.; Pham, T. M.; Chi, S. C.; Nguyen, H. A.; Bui, Q. D.; Bui, D. N.; Tran, T. Q. Effect of surfactant on the in vitro dissolution and the oral bioavailability of a weakly basic drug from an amorphous solid dispersion. *Eur. J. Pharm. Sci.* **2021**, *162*, 105836. DOI: 10.1016/j.ejps.2021.105836.
- Aroso, I. M.; Silva, J. C.; Mano, F.; Ferreira, A. S. D.; Dionísio, M.; Sá-Nogueira, I.; Barreiros, S.; Reis, R. L.; Paiva, A.; Duarte, A. R. Dissolution enhancement of active pharmaceutical ingredients by therapeutic deep eutectic systems. *Eur. J. Pharm. Biopharm.* **2016**, *98*, 57–66. DOI: 10.1016/j.ejpb.2015.11.002.
- Gao, Y.; Glennon, B.; Kamaraju, V. K.; Hou, G.; Donnellan, P. Dissolution kinetics of a BCS class II active pharmaceutical ingredient. *Org. Process Res. Dev.* **2018**, *22* (3), 328–336. DOI: 10.1021/acs.oprd.7b00365.
- Lentz, K. A.; Plum, J.; Steffansen, B.; Arvidsson, P. O.; Omkvist, D. H.; Pedersen, A. J.; Sennbro, C. J.; Pedersen, G. P.; Jacobsen, J. Predicting in vivo performance of fenofibrate amorphous solid dispersions using in vitro non-sink dissolution and dissolution permeation setup. *Int. J. Pharm.* **2021**, *610*, 121174. DOI: 10.1016/j.ijpharm.2021.121174.
- Prajapati, N.; Späth, M.; Knecht, L.; Selzer, M.; Nestler, B. Quantitative phase-field modeling of faceted crystal dissolution processes. *Cryst. Growth Des.* **2021**, *21* (6), 3266–3279. DOI: 10.1021/acs.cgd.0c01715.
- Wei, Y.; Zhang, L.; Wang, N.; Shen, P.; Dou, H.; Ma, K.; Gao, Y.; Zhang, J.; Qian, S. Mechanistic study on complexation-induced spring and hover dissolution behavior of ibuprofen-nicotinamide cocrystal. *Cryst. Growth Des.* **2018**, *18* (12), 7343–7355. DOI: 10.1021/acs.cgd.8b00978.
- Najib, M.; Hammond, R. B.; Muhmud, T.; Izumi, T. Impact of structural binding energies on dissolution rates for single

- faceted-crystals. *Cryst. Growth Des.* **2021**, *21* (3), 1482–1495. DOI: 10.1021/acs.cgd.0c01142.
11. Chen, D.; Sun, Q.; Huang, W.; Yang, B. Diverse solvent selection for polymorph landscape investigation based on specific API–solvent interactions. *Cryst. Growth Des.* **2020**, *20* (4), 2251–2265. DOI: 10.1021/acs.cgd.9b01380.
 12. Elts, E.; Greiner, M.; Briesen, H. Predicting dissolution kinetics for active pharmaceutical ingredients on the basis of their molecular structures. *Cryst. Growth Des.* **2016**, *16* (7), 4154–4164. DOI: 10.1021/acs.cgd.6b00721.
 13. Opio, C. K.; Lee, W. M.; Kirkpatrick, P. Entecavir. *Nat. Rev. Drug Discov.* **2005**, *4* (7), 535–536. DOI: 10.1038/nrd1780.
 14. Cho, H.; Ahn, H.; Lee, D. H.; Lee, J. H.; Jung, Y. J.; Chang, Y.; Nam, J. Y.; Cho, Y. Y.; Lee, D. H.; Cho, E. J.; et al. Entecavir and tenofovir reduce hepatitis B virus-related hepatocellular carcinoma recurrence more effectively than other antivirals. *J. Viral Hepat.* **2018**, *25* (6), 707–717. DOI: 10.1111/jvh.12855.
 15. Xu, H.; Wang, F.; Xue, W.; Zheng, Y.; Wang, Q.; Qiu, F. G.; Jin, Y. Total synthesis of entecavir: a robust route for pilot production. *Org. Process Res. Dev.* **2018**, *22* (3), 377–384. DOI: 10.1021/acs.oprd.8b00007.
 16. Kang, Y.; Shao, Z.; Wang, Q.; Hu, X.; Yu, D. Quantitation of polymorphic impurity in entecavir polymorphic mixtures using powder X-ray diffractometry and Raman spectroscopy. *J. Pharm. Biomed. Anal.* **2018**, *158*, 28–37. DOI: 10.1016/j.jpba.2018.05.026.
 17. Ding, Y.; Dong, L.; Zhou, J. P. [Comparative study on quality of entecavir tablets] [Article in Chinese]. *Chung Kuo Yao Hsueh Tsa Chih* **2015**, *50* (1), 58–62.
 18. Francis, A. T.; Nguyen, T. T.; Lamm, M. S.; Teller, R.; Forster, S. P.; Xu, W.; Rhodes, T.; Smith, R. L.; Kuiper, J.; Su, Y.; Fu, D. In situ stimulated Raman scattering (SRS) microscopy study of the dissolution of sustained-release implant formulation. *Mol. Pharm.* **2018**, *15* (12), 5793–5801. DOI: 10.1021/acs.molpharmaceut.8b00965.
 19. Yan, L.; Yinghua, S.; Shang, W.; Zhonggui, H. [Determination of equilibrium solubility of entecavir and its apparent oil/water partition coefficient by HPLC] [Article in Chinese]. *Chinese J. Pharma.* **2014**, *12* (6), 201–207. DOI: 10.14146/j.cnki.cjp.2014.06.004.
 20. Noyes, A. A.; Whitney, W. R. The rate of solution of solid substances in their own solutions. *J. Am. Chem. Soc.* **1897**, *12* (19), 930–934. DOI: 10.1021/ja02086a003.